Journal of Geoscience and Environment Protection, 2024, 12, 284-306
https://www.scirp.org/journal/gep
ISSN Online: 2327-4344
ISSN Print: 2327-4336

Application of Remote Sensing in Coral Reef Mapping and Assessment of Climatic and Environmental Conditions

Amina Said[1], Mark Boitt[2], Michael Hahn[1]

[1]Faculty of Geomatics, Computer Science and Mathematics, Hochschule fuer Technik Stuttgart, Stuttgart, Germany
[2]Institute of Geomatics, GIS and Remote Sensing, Dedan Kimathi University of Technology, Nyeri, Kenya
Email: am.omarsaid@gmail.com, michael.hahn@hft-stuttgart.de, mark.boitt@dkut.ac.ke

How to cite this paper: Said, A., Boitt, M., & Hahn, M. (2024). Application of Remote Sensing in Coral Reef Mapping and Assessment of Climatic and Environmental Conditions. *Journal of Geoscience and Environment Protection, 12,* 284-306.
https://doi.org/10.4236/gep.2024.1211016

Received: November 20, 2023
Accepted: November 26, 2024
Published: November 29, 2024

Copyright © 2024 by author(s) and Scientific Research Publishing Inc.
This work is licensed under the Creative Commons Attribution International License (CC BY 4.0).
http://creativecommons.org/licenses/by/4.0/

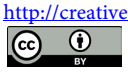

Open Access

Abstract

Coral reefs have tremendous benefits to both humans and marine biodiversity but are globally endangered. Traditionally, data collection of coral reefs was field-work based, which is time-consuming, costly and lacking in full coverage. This study shows that optical imageries can be utilised to map coral reefs, by fusing visible bands and depth invariant index (DII) to classify benthic features. Overall accuracy of at least 68 percent is achieved. However, to overcome the challenge of cloud cover, which is common in coastal areas, microwave imagery is used to map the emergent coral reefs. Again, remote sensing proves to be reliable in estimation of sea surface temperature (SST) and extraction of water quality parameters through Case-2 Region CoastColour (C2RCC) processor. Thereafter, regression analysis is performed to evaluate the correlation of SST and water quality. It is concluded that higher spatial resolution can improve coral mapping and that there is a need for more research on correlation to its environment.

Keywords

Coral Reef, DII, SST, C2RCC, Water Quality

1. Introduction

Coral reefs are majorly tropical and some are semi-tropical marine species that grow in salty water. They grow optimally between temperatures of 23 - 29 degrees Celsius (NOAA, 2021). Despite covering less than one percent of the ocean floor, tropical coral reefs provide support to 25 percent of the only known marine species (Hoegh-Guldberg et al., 2017). Coral reefs play an important role in marine biodiversity, and they provide habitat and breeding ground for a variety of marine

organisms. These organisms provide food and income for coastal people, which in return relates to implementation of Blue Economy agenda. In addition, coral reefs have a great benefit to the environment as they protect coastlines from damage and erosion due to effects of storm surges and waves (Coral Reef Alliance, 2021). Furthermore, they promote recreational activities such as snorkelling and diving. This boosts tourism not only locally but globally as well (Conservation Education Society, 2021). The international tourism acts as one of the important sources of foreign exchange earners in Kenya. Therefore, it contributes to the development of economy of the country. Last but not least, coral reefs are a vital resource in pharmaceutical development (Hoegh-Guldberg et al., 2017). It is commonly used in medical research as well as in treatment. In summary, due to their great support of marine biodiversity and its other benefits, they are referred to as the rainforests of the sea (Budi Cahyono et al., 2020). Traditionally, data collection for research on coral reefs was carried out through in situ observations. This involved divers, who were guided by transect lines, quadrants, towing boats, etc. to collect data on the coral reefs. The data is then recorded on water-proof notebooks, which makes it prone to gross errors. This method proved to be time-consuming and costly, and it lacked full coverage of coral reefs. Moreover, underwater photogrammetry techniques have also been adopted in mapping of coral reefs. Close range photogrammetry has been used in mapping the coral reefs in detail. This technique has been used together with structure from motion (SfM) to generate three-dimensional (3D) visualisations, whereby texture of coral reefs is also mapped. Budi Cahyono et al. (2020) found that utilising photogrammetry to create 3D models of coral reefs is possible. However, since the corals behave like a tree branch, holes appeared in the model. The holes can be solved by increasing the number of photos used in creating the 3D model. This will not only be more expensive but also more time-consuming. Additionally, as opposed to underwater photogrammetry, unmanned aerial vehicles (UAVs) have also been adopted into benthic mapping using photogrammetry and SfM. Casella et al. (2017) suggested a technique in creating 3D models of coral reefs but in small scale using drone. The study found that the atmospheric and water conditions restricted the application of this technique. However, its coverage scale lies between the underwater photogrammetry and remote sensing. Again, this method can be time-consuming for a large area as well as expensive.

Thus, remote sensing has been found to be a fast and cost-effective technique in carrying out coral reef studies. However, just like the photogrammetry techniques, there is limitation of capturing data beyond certain depth of water and is dependent on transparency of water. With the development and advancement of geospatial technology, it is anticipated fusion of the various techniques will be used to provide coral reef maps and models on varying scale. That is, remote sensing can be adopted to do coarse mapping of the coral reefs. This can then be supplemented by utilising the photogrammetry techniques to provide fine-detailed maps and models.

The objective of the study is to map coral reefs and correlate them to water quality parameters and SST. SST and pollution are two of the major threats facing coral reefs. Thus, the study aims at providing an understanding of the influencing factors of coral reef growth and flourishment, which will assist in not only managing vital resources, but also in frequent monitoring.

2. Study Area and Data

2.1. Study Area

The area of study is Malindi and Watamu marine protected areas (MPAs), found in Kilifi County of Kenya as shown on a map in Figure 1. Kilifi neighbours the second largest city in Kenya, Mombasa. Spatially it lies around 3.51˚ south and 39.90˚ east. It has temperatures ranging between 20 and 33 degrees celsius. The study area is approximately 7 km away from the river mouth of the second longest river in Kenya. This river has three different names, commonly known as river Athi-Galana-Sabaki. The names are based on the region and course of the river, the lower course feeding into the ocean is known as Sabaki. Moreover, the study area is close to both terrestrial and marine forests of Arabuko-Sokoke and Mida Mangroves respectively. The coastline along the study area is dominated by sandy, clay and loam soils (CIAT, 2016).

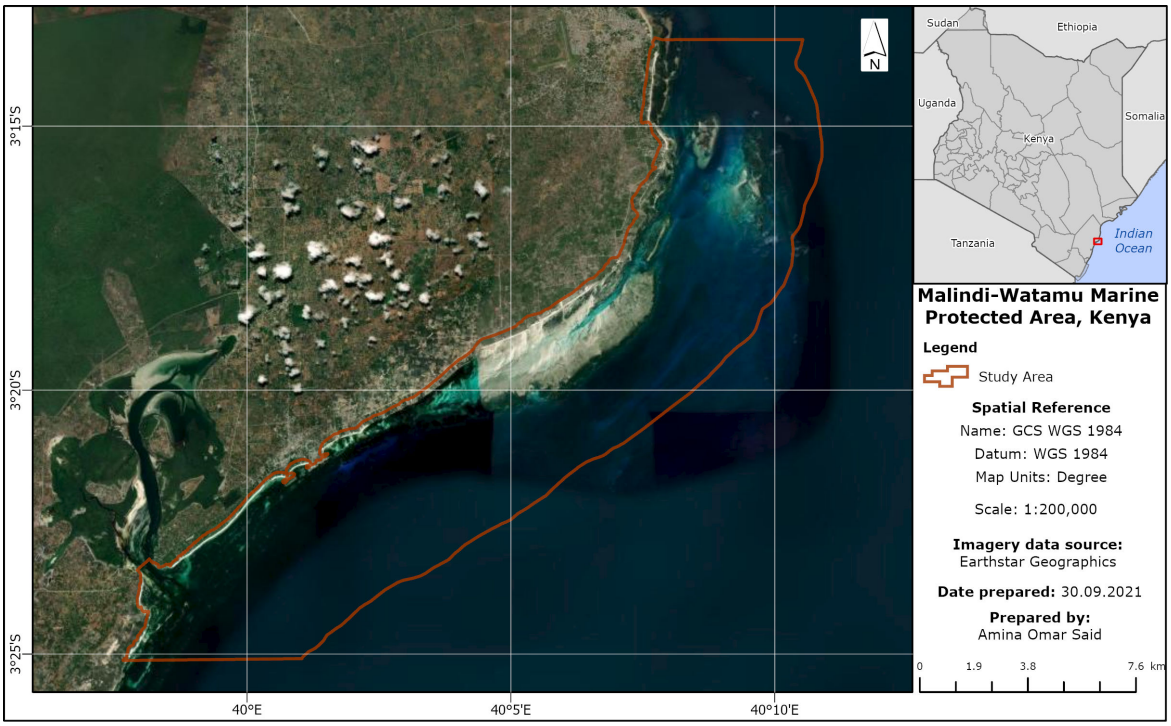

Figure 1. Map showing the Malindi and Watamu marine protected areas.

The area is known for its beautiful oceanic sceneries and is also close to important historical sites. It is one of the major tourist destinations in Kenya. The main economic activities are tourism, fishing, mining and trade.

2.2. Relevant Data

Satellite imageries are used to carry out the study of the coral reefs. Table 1 shows the data used.

Table 1. Satellite data, source, spatial resolution and launch date.

Data	Source	Resolution (m)	Launch Date
Sentinel-1	ESA	10	April 2014
Sentinel-2	ESA	10	June 2015
Landsat-8 (TIR)	NASA	100	February 2013

The data used is open data of Sentinel-1 and 2 imageries from European Space Agency (ESA) and Landsat-8 from National Aeronautics and Space Administration (NASA). Modis-Terra and Sentinel-3 imageries are used to validate the water quality parameters for 2016 and 2020 respectively. Modis-Terra has a spatial resolution of 4 km, while Sentinel-3 has a spatial resolution of 300 m. Sentinel-3 focuses on providing data for marine studies. It provides a vast range of data on marine, such as SST and the water quality parameters. It provides SST data at a spatial resolution relatively higher than most of other satellite platforms. Level-4 data of Group for High Resolution Sea Surface Temperature (GHRSST) of 1 km spatial resolution is used to validate the mapped SST for both temporal periods.

3. Methodology

Figure 2 shows the flowchart of the methodology that was adopted for this study.

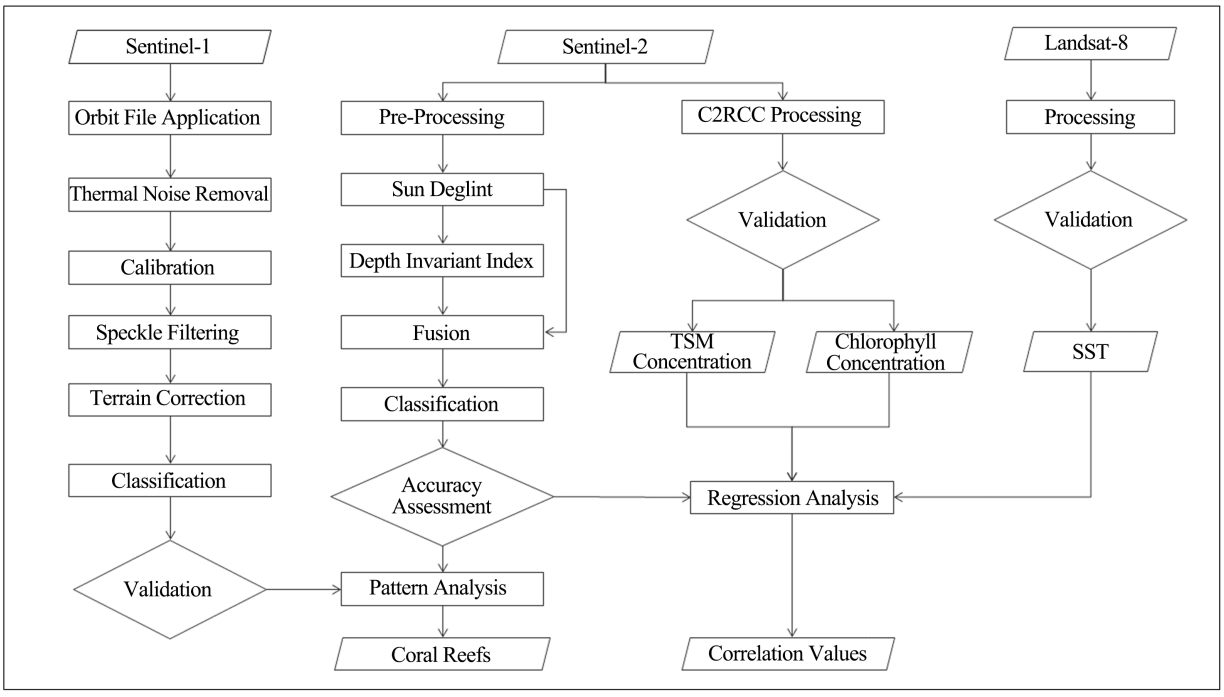

Figure 2. Methodology flow chart.

3.1. Sea Surface Temperature (SST)

Landsat-8 is used for extracting the surface temperature of the sea. Band-10 of TIR with spatial resolution of 100 m is of interest in computation of the surface temperature. For processing, subset with respect to study area and masking of land surface is carried out. Since the data is of level-2 with atmospheric corrections, no further processing is necessary. Thereafter, the surface temperature is estimated. The surface temperature is calculated using scale factor shown in Equation (1) (USGS, 2022).

$$\text{Surf. temp.,}\ ^{\circ}\text{C} = \left(\left(\text{B10} \times 0.00341802\right) + 149.0\right) - 273.15 \quad (1)$$

Consequently, the accuracy of the SST estimate is assessed using level-4 SST data of GHRSST, which has a spatial resolution of 1 km (Chin, Vazquez-Cuervo, & Armstrong, 2017). SST values of both Landsat-8 and GHRSST are extracted onto the sampling points and statistical assessment is carried out. The statistical values are evaluated to ascertain the accuracy of the surface temperature estimates.

3.2. Water Quality

Water quality parameters are used to analyse level of water pollution in the study area. This includes the chlorophyll and TSM concentrations. Due to its higher spatial and temporal resolutions, Sentinel-2 is preferred over Sentinel-3 for extraction of water quality parameters for this study. C2RCC processor is used to extract chlorophyll and TSM concentration values. For C2RCC processor, level-1 data with atmospheric biases is used as an input. The atmospheric correction and derivation of water quality parameters is carried out simultaneously. The accuracy of the parameters for 2016 is evaluated by comparing the derived values of Sentinel-2 with Modis-Terra, while Sentinel-3 is used to validate the 2020 water quality parameters. The statistical measures are analysed to ensure the estimates of the parameters are consistent and acceptable for analysis.

3.3. Synthetic Aperture Radar (SAR)

Geometric and radiometric corrections are carried out on the SAR imageries to account for errors due to incorrect geometric orientation and signal noises. This constitutes a series of steps and are discussed below.

3.3.1. Data Pre-Processing

The first step is application of orbit file to ensure the right position, velocity and metadata of the scenes are used. Secondly, elimination of thermal noise that is common in cross polarized SAR imageries. The thermal noise is particularly common when the backscatter energy is low (Park et al., 2018). Thus, the noise tends to overestimate the backscatter values. After that, calibration is done to account for radiometric biases and errors. This process converts the value of pixels from digital numbers (DN) to precise backscatter values (Filipponi, 2019). Thus, the data is converted from level-1 to level-2, giving the actual backscatter values without radiometric biases. Following is speckle filtering, to get rid of the noise that is

generated due to interference of the returning waves (backscatter waves). The speckle noise causes effect of salt and pepper on the imagery, which affects appearance of imagery and accuracy of the analysis. Filters which have provided good speckle filtering results, i.e., the Gamma Map, Lee and Frost filters (Rudorff & Gherardi, 2008) are compared. Lee filter is the most common and found to be superior (Filipponi, 2019) for visual analysis and interpretation. Of interest in this study is to reduce the speckle noise while still maintaining the sharpness of edges of the features on the imagery. So as to assist in not filtering out any tiny but significant detail, which is essential in identifying the exposed reefs. Then, terrain correction is carried out to compensate for the geometric errors during acquisition of data. This is caused by the side-looking characteristic of SAR platforms which not only affects the orientation of the imagery but also the ground distance (Filipponi, 2019). Next, subset is done using the specified bounding box parameters defined for the study area. This is to reduce the bulkiness of data for fast processing. Moreover, ensures focus of analysis is only on study area to avoid disturbance by neighbouring and unwanted features. Lastly, masking of land surface to remove the backscatter values of land surface. This improves the classification results and subsequently the identification of exposed reefs.

3.3.2. Classification Algorithms

Two unsupervised classification algorithms are tested to assess the results: expectation maximization (EM) cluster analysis and K-Means. The number of classes defined is two classes: first is to represent the water surface and second is for a combination of waves and exposed reefs. The result of speckle filters which provides better output among the three is used in classification of the processed data using EM cluster and K-Means classifiers. This is to further compare the filters based on noise, edge sharpness and simplification.

3.3.3. Change Analysis

To support the validation of existence of exposed reef, change detection is carried out. Imageries of 2016 and 2020 are used for the change analysis. It is expected that exposed reefs are visible in both temporal periods. However, the level of exposure varies depending on the changing sea tides.

3.4. Multispectral Imagery

The main multispectral data used is the Sentinel-2 satellite imageries. Level-1 imageries of 2016 and 2020 with atmospheric biases. This involves various steps from data collection, processing, bands fusion, classification and accuracy assessment. Data collection and processing is discussed below in detail.

3.4.1. Data Collection and Processing

Satellite imageries are sourced from ESA. A keen interest is finding imageries with no or less than 10 percent of cloud cover for the study area. This ensures the data is eligible for mapping and analysis. Good data coverage of study area assists in

achieving the study aim. The processing involves several steps and are discussed below.

Atmospheric correction—this is carried out on level-1 imageries using Sen2Cor and C2RCC tools in SNAP to upgrade the level-1 data to level-2. Thus, the reflectance values are converted from the top of atmosphere (TOA) to bottom of atmosphere (BOA). This process ensures the reflectance values are more precise with respect to the actual reflectance of the features, without influence due to atmospheric biases and errors. Resampling of Sentinel-2 imagery which has 13 bands with spatial resolution ranging from 10 m to 60 m. The visible bands (blue, green and red) and near infrared (NIR) band have a resolution of 10 m, while the lowest resolution is of band 1 (blue aerosols) and band 10 (cirrus) with a spatial resolution of 60 m. Hence, upsampling resampling is done to simplify the processing of the imagery by having a standard pixel size for all bands. This procedure converts the relatively low spatial resolution bands of the imagery, to a spatial resolution of the defined reference band. Thus, more pixels are produced from the low spatial resolution bands and increasing data storage capacity. This ensures all pixels of different bands have the same spatial resolution. This promotes not only bands consistency but also improves the analysis. The resampling is carried out using band 2 of Sentinel-2 as a reference band, with a spatial resolution of 10 m.

Subset of Sentinel-2 imageries with respect to the area of interest, which fully covers Malindi and Watamu MPAs. This is done to ensure that only the area of interest is covered, so as to reduce the data capacity and the processing time. This also assists in removal of noise, which affects the data and eventually impacts the accuracy of analysis results.

Sun deglint processing is carried out next. Since the water is unstill, the effects of sun glint are visible on the imageries. To facilitate easier and quicker identification of sun glint effects for removal, band 8 of NIR is used. The deglint also masks unwanted areas on imagery, such as the land area, clouds and its shadow. Equation (2) shows the formula used for deglint processing (Hedley, Harborne, & Mumby, 2005).

$$R_i' = R_i - b_i \left(R_{NIR} - Min_{NIR} \right) \tag{2}$$

where R_i' = radiance in image with sun glint;

R_i = radiance in band i;

b_i = regression slope;

R_{NIR} = radiance value of NIR band;

Min_{NIR} = minimum radiance of NIR band.

Land Cloud White Cap Mask follows to mask areas that are previously unmasked. It filters out unmasked clouds and their shadows. A suitable threshold is set to ensure most of the clouds and the shadows are masked without masking the sea surface.

3.4.2. Depth Invariant Index (DII)

The DII is generated using band 2 and band 3 of processed imageries. Polygons of

two feature types are drawn: one is area of the same bottom type, in this case the sandy areas. Second is deep-water areas which are areas which appear as dark blue on the imagery. Thus, the two bands and polygons representing deep-water and sand areas are used as input to generate the DII values.

3.4.3. Band Fusion

Each of the DII layer generated is stacked with the respective MS imageries used in creating the respective DII layer. Hence, for 2016 MS imagery, the four bands processed i.e., band 2 to band 5 are stacked with the DII layer of 2016. Bands of longer wavelength are preferred due to their better penetration power into water. The same is done to 2020 data, however band 1 is also integrated into the fused data. Incorporating the two data into one for classification improves the classification results.

3.4.4. Classification of Marine Features

The interest is on classification and mapping of not only coral reef, but also its neighbouring features such as sand, seagrass and mixed areas. This is done to assist in understanding the distribution of coral reefs, as well as its association with its surrounding marine features.

Segmentation of Sentinel-2 is carried out to create clusters of pixels representing the various features. This is followed by creating training points for the feature classes. Thereafter, the zonal statistics of the segments is created to have estimates of the reflectance values of the segments. Joining of training points with zonal statistics follows, to get average estimates of reflectance for the points. The trained vector is then classified, thus classification of the segments with respect to the trained feature classes is carried out.

Additionally, unsupervised classification is carried out using the fused data. EM cluster and K-Means classifiers are used for classification and comparison. Thirty iterations are input, with the number of classes varying between 10 - 15. The results of the various numbers of classes are compared and analysed. The allocation of features to the classes is based on visual interpretation of the imagery. This is compared to high spatial resolution imageries of Google Earth.

3.4.5. Accuracy Assessment

For accuracy, random stratified sampling technique is deployed. Grids covering the study area are created and for each grid, one random point is generated. The distribution of the sampling points is analysed and verified. This ensures there is a good representation of sampling points not only across the whole study area, but also across all features present. As a result, it helps in reducing biases towards features of small geometric coverage. Points that fall away from study or masked area are not considered. The accuracy of the results is evaluated by comparing classified features and the mapped features of the validation data. The user accuracy, producer accuracy, overall accuracy and kappa coefficient are calculated and the reliability of the classification results assessed.

4. Results and Discussion

This chapter presents the findings of the study and its evaluation. This involves an in depth analysis of the results, intending to provide an understanding of the findings. Moreover, this will assist in identifying gaps that may require further research and study.

4.1. Sea Surface Temperature (SST)

Figure 3 shows the average monthly SST for the study area. Figure 4 shows the SST for 2016 and 2020 respectively that the SST is higher in 2016 as compared to 2020. The surface temperatures range between 29 - 48 and 25 - 36 degrees celsius for 2016 and 2020 respectively. Areas that are closer to the coastline have higher SST as compared to areas further away. The SST tends to increase towards the coastline due to more solar energy penetrating through the water (Daud et al., 2019). Areas that are away from coastline are relatively cooler with slightly lower SST.

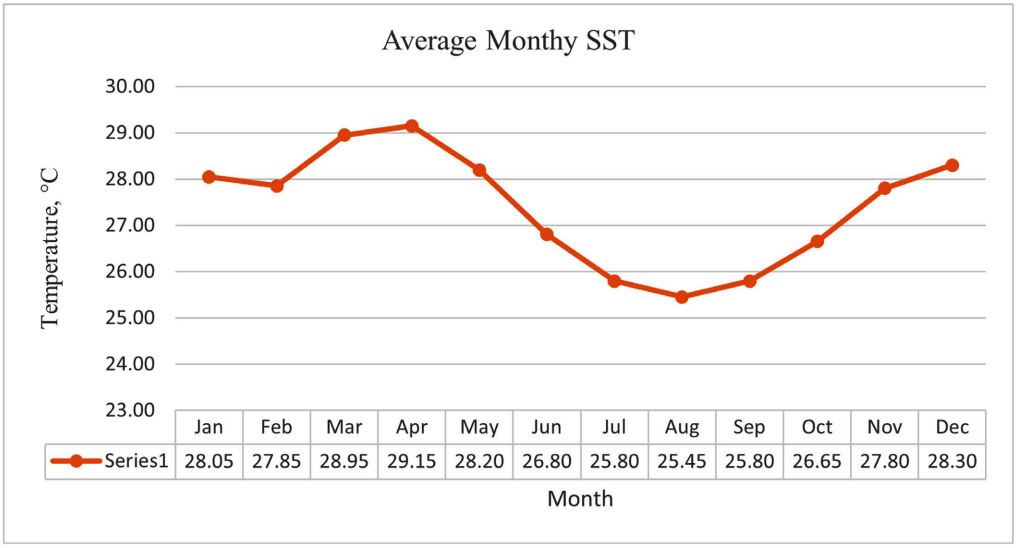

Figure 3. Average monthly SST for the study area.

The average is calculated using past SST records of the area. The figure presents April as the hottest month of the year with 29˚C and August as the coolest with about 26˚C. March is the second hottest month with close to 29˚C, while June is forth coolest month with almost 27˚C. The surface temperature is higher in 2016 as compared to 2020, due to difference of seasons. Furthermore, the higher SST of 2016 is contributed by El Nino event of 2015/2016 (NASA Earth Observatory, 2017).

The validation results of both temporal periods have a small difference and the root mean square errors (RMSEs) are around one degree celsius for both epochs. The RMSE is 0.94˚C and 1.03˚C for March 2016 and June 2020 respectively. The difference between the SST from Landsat-8 and GHRSST is relatively good,

despite the huge difference of spatial resolution of the data. Moreover, this proves that SST values attained from Landsat-8 are reliable and GHRSST values can equally be considered for future studies.

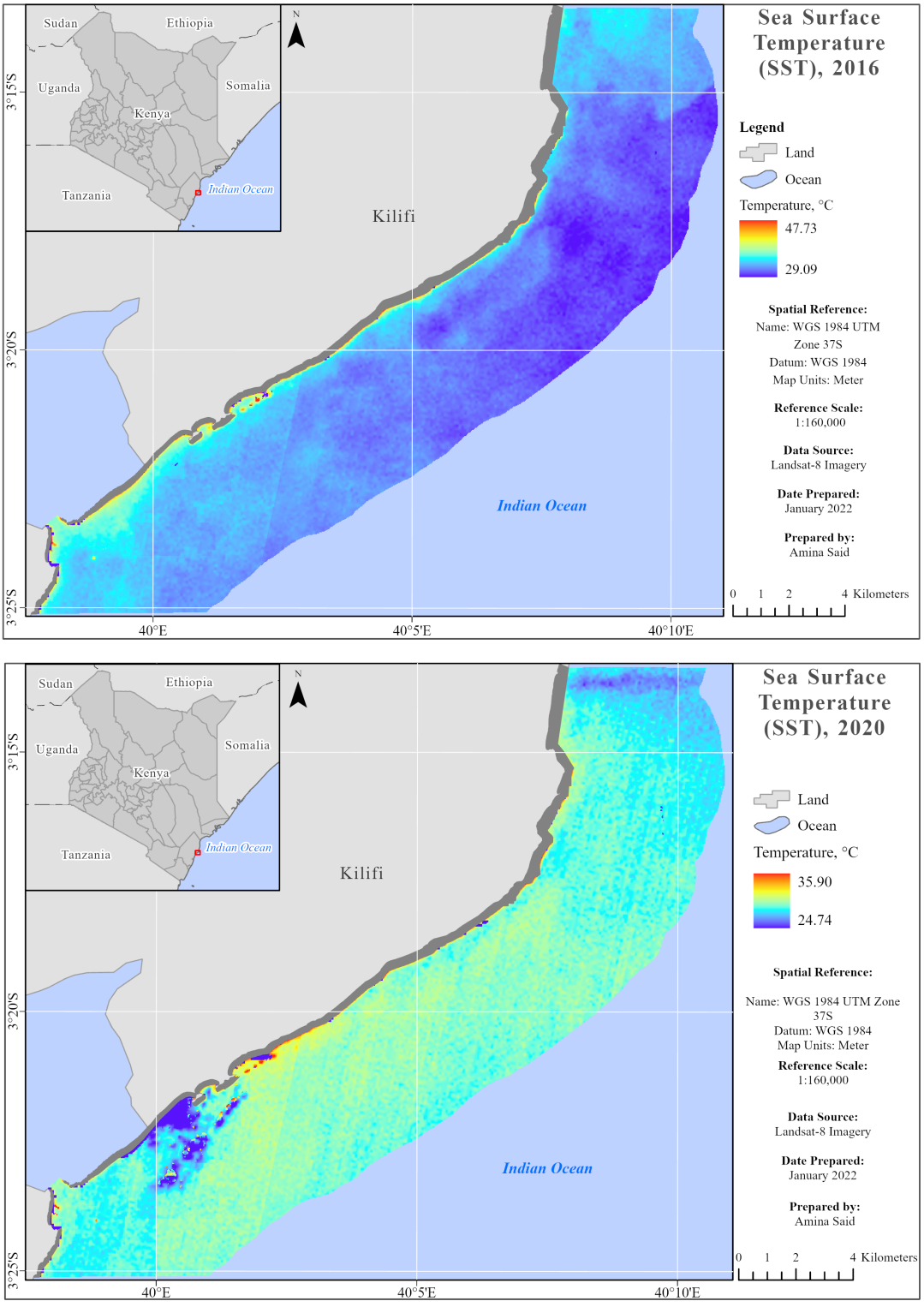

Figure 4. Sea surface temperature in 2016 and 2020 respectively.

Gomez et al. (2020) carried out to a study to compare the satellite SST and in situ temperature at the coral depth. Three different satellites data were compared to the in-water temperature data. The findings show that a strong correlation of greater than 0.90 exists between satellite SST and in situ data. However, satellite data underestimates the actual temperature at depth with about one degree Celsius. The temperature difference is proportional to depth, thus shallower coral reefs have a stronger correlation to SST than deeper ones. This implies surface temperatures from satellite imagery may be relied on for coral studies. Since satellite imageries are used to map shallow water coral reefs and thus have a good correlation between actual and satellite-derived temperature. In summary, this indicates that despite the differences of spatial resolution and seasons, there is a good consistency of SST estimated by various satellites and in situ data. This is quite useful and a cheaper method in estimation of in water temperature of coral reefs for monitoring and analysis.

4.2. Water Quality

Figure 5 shows the distribution of chlorophyll concentration for the year 2016 and 2020. The values range from almost negligible amount to approximately 54.00 mg/m^3 for both periods. However, the high concentrations are more spread in 2016 than in 2020 as can be seen in Figure 5. For 2016, the highest concentration cluster of range of 9.40 - 54.00 mg/m^3 is dominating and spread across the area. While in 2020, the first two clusters of lowest concentration range of 0.01 - 0.61 and 0.62 - 3.59 mg/m^3 are dominating in the study area.

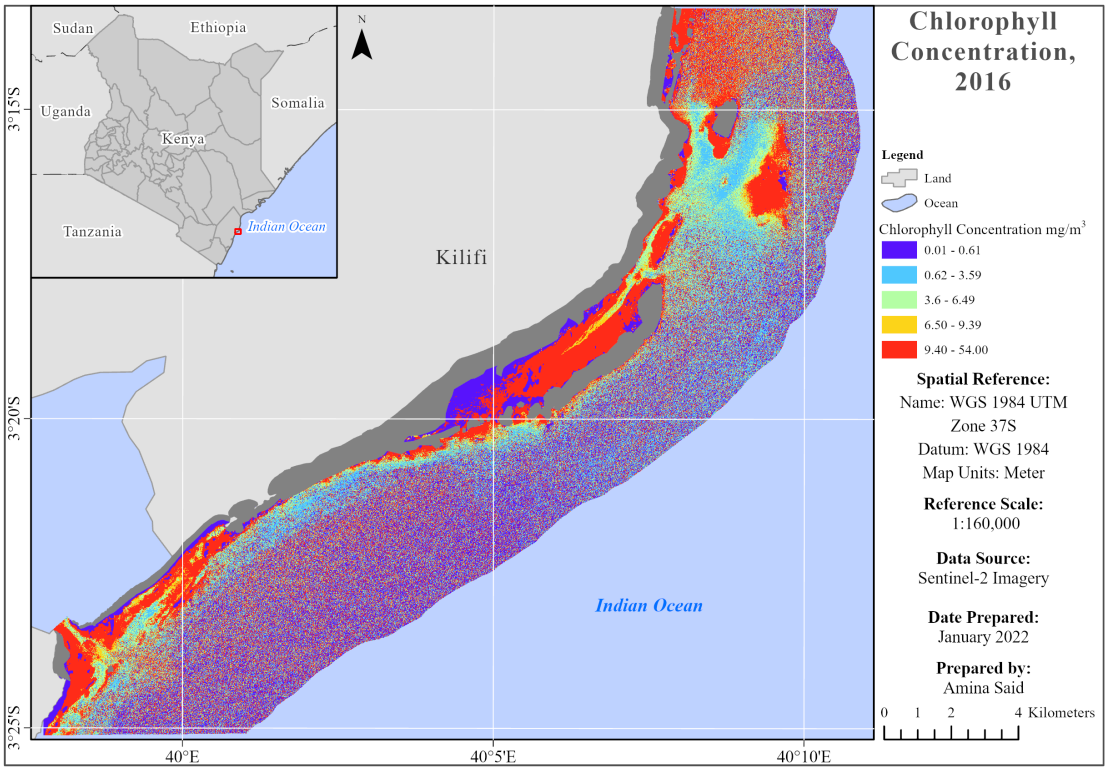

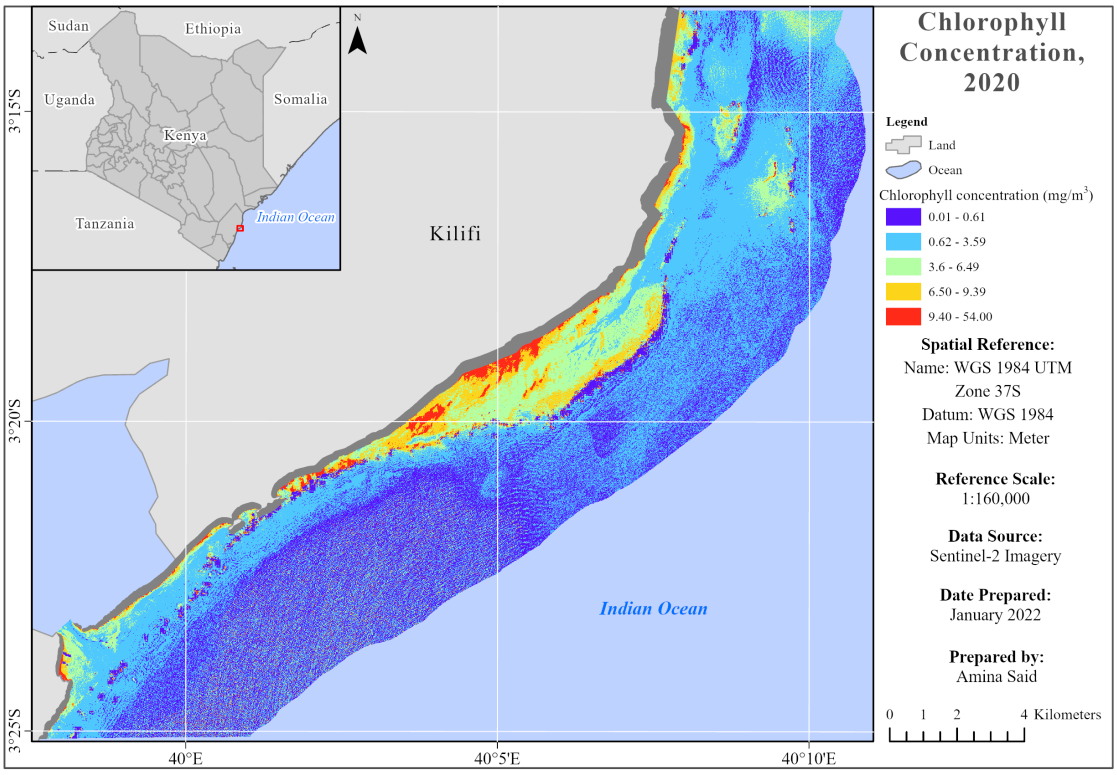

Figure 5. Chlorophyll concentration in 2016 and 2020 respectively.

Figure 6 shows the distribution of TSM concentration for the year 2016, the values range between 0.01 g/m^3 and 49.49 g/m^3. The range that is widespread in 2016 is second lowest concentration cluster of 1.30 - 9.00 g/m^3. The coastline has the second cluster dominating and more of the higher concentration values as compared to other parts of the study area. The two lowest concentration clusters are more common in areas away from the coastline and towards the deep sea. Figure 6 indicates that the distribution of TSM concentration in 2020, is ranging between 0.01 - 49.49 g/m^3. The dominating values are of cluster with the lowest concentration values of 0.01 - 1.29 g/m^3, which is mainly away from the coastline. Again for 2020, the second cluster of concentration values between 1.30 g/m^3 and 9.00 g/m^3 spreads along the coastline just like in 2016. However, unlike 2016, the coastline does not contain the upper clusters of TSM concentrations. Nevertheless, the TSM concentration values are within good water quality concentrations for both periods.

As it has been seen, there is a difference of both TSM and chlorophyll concentration values between the two periods. March 2016 has a relatively higher concentration as compared to June 2020. Sent et al. (2021) analysed monthly water quality parameters, the study found that the concentrations are higher in summer and spring seasons. As previously discussed in SST, March is part of the hottest season of the study area. While June is part of the cool season, thus the relatively lower temperature. Nima et al. (2016) also observed the seasonal variations of chlorophyll concentrations in a study carried out in Norwegian coastal water.

Maximum chlorophyll concentrations are reported in July, during the summer season. This explains the tremendous difference of chlorophyll concentration values between the two periods of different seasons.

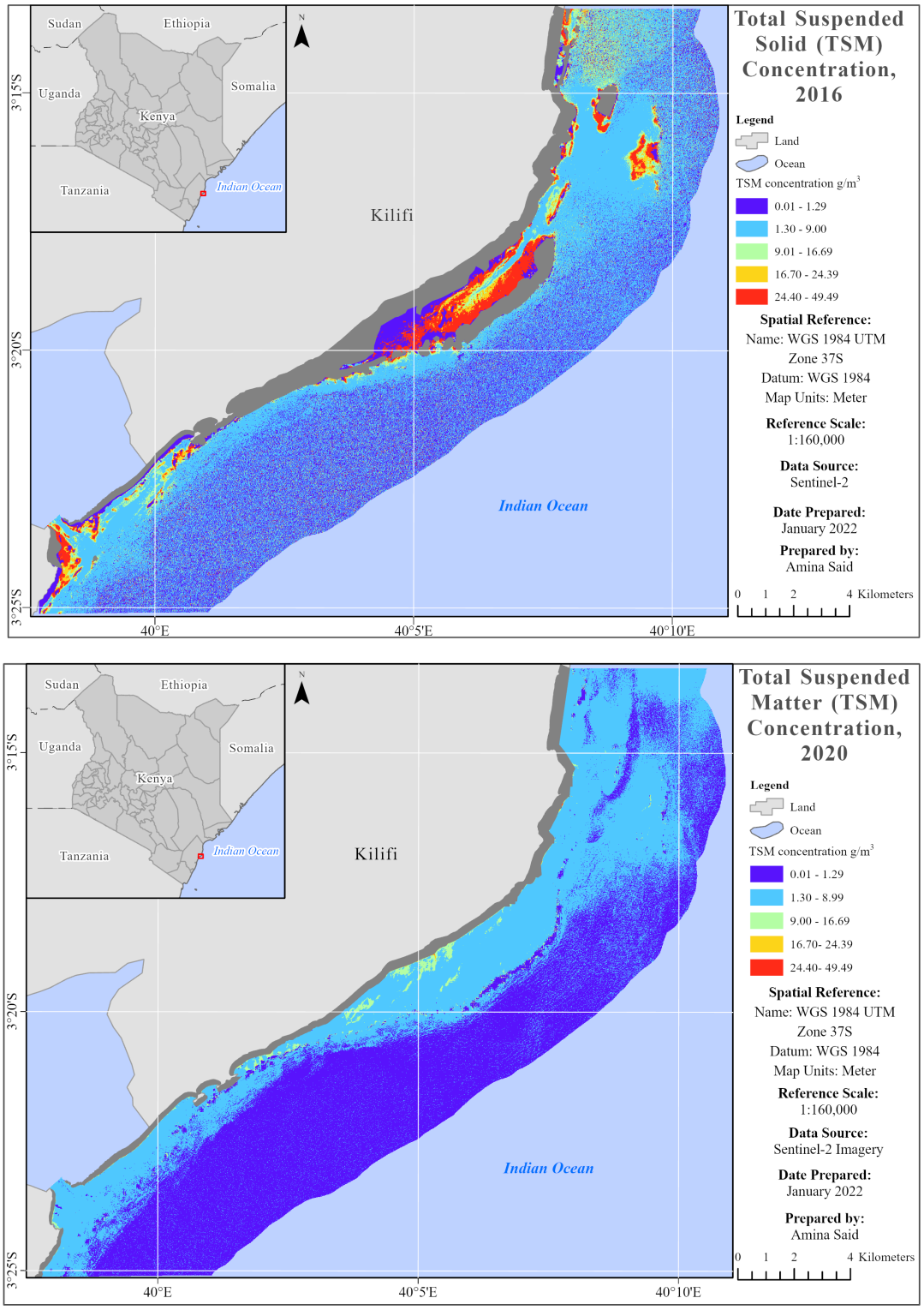

Figure 6. TSM concentration in 2016 and 2020 respectively.

Another observation is made on pattern of distribution of the high concentration values of TSM and chlorophyll for both temporal periods. Areas closer to the land tend to have relatively higher values as compared to areas further away from shoreline (Daud, Pin, & Handayani, 2019). Again, these variations are significant between the two temporal periods. Sent et al. (2021) observed that the seasonal pattern of differences of water quality parameters is more visible around estuaries. Hence, the inner estuaries have higher seasonal variations. A similar observation is made in this study for the area closer to the coastline. This is also more noticeable on the lower left part of the coastline for 2016 chlorophyll values. The area has high concentration values, as the coastline branches into Mida Creek.

It is noted that there is a trend between the water quality parameters and their uncertainties. Where the concentrations are mapped as high, uncertainty values are also mapped as high. This is due to the fact that as the concentration increases, it is less likely to be identified by the sensor (La Yasir Haya & Fujii, 2017). This is due to the concentration values being inversely proportional to light penetration into the water and thus recognition by satellites. As the water quality parameters increase, it affects the water clarity and thus light penetration. A correlation is observed to exist between the TSM and chlorophyll concentration values. Hence regression analysis is carried out to evaluate the relationship that exists between TSM and chlorophyll concentrations.

4.3. SAR Classification

On comparing results of K-Means and EM Cluster unsupervised classification algorithms, EM Cluster provides better results as compared to K-Means. The classification results of KMeans has more noise on sea surface as compared to EM Cluster. It is also observed that the classification result of Gamma Map filter has much less noise as compared to Lee filter classification result. Thus, EM Cluster provides better results in identifying the exposed reefs and effects of waves without including much noise. However, from elimination of noise, it may underestimate the exposed reefs. Furthermore, EM Cluster is considered when carrying out classification of unstable environments such as of water surface (Korting et al., 2007). Thus, the results from Gamma Map filter and EM-Cluster are used for the final identification of the emergent reefs.

Figure 7 shows the exposed reefs as linear features running along the coastline. The reef distance from the coastline varies and it decreases as it moves towards the south. Based on the characteristics it exhibits; the reefs categorise as barrier reefs.

Such reefs run parallel to the shoreline and form a borderline (Zanga et. al., 2019). This creates a lagoon, which separates the reef from the shoreline (Kennedy & CR, 2020). Large barrier reefs are unique and the most commonly known reef of this type is The Great Barrier Reef of Australia (Zanga et. al., 2019).

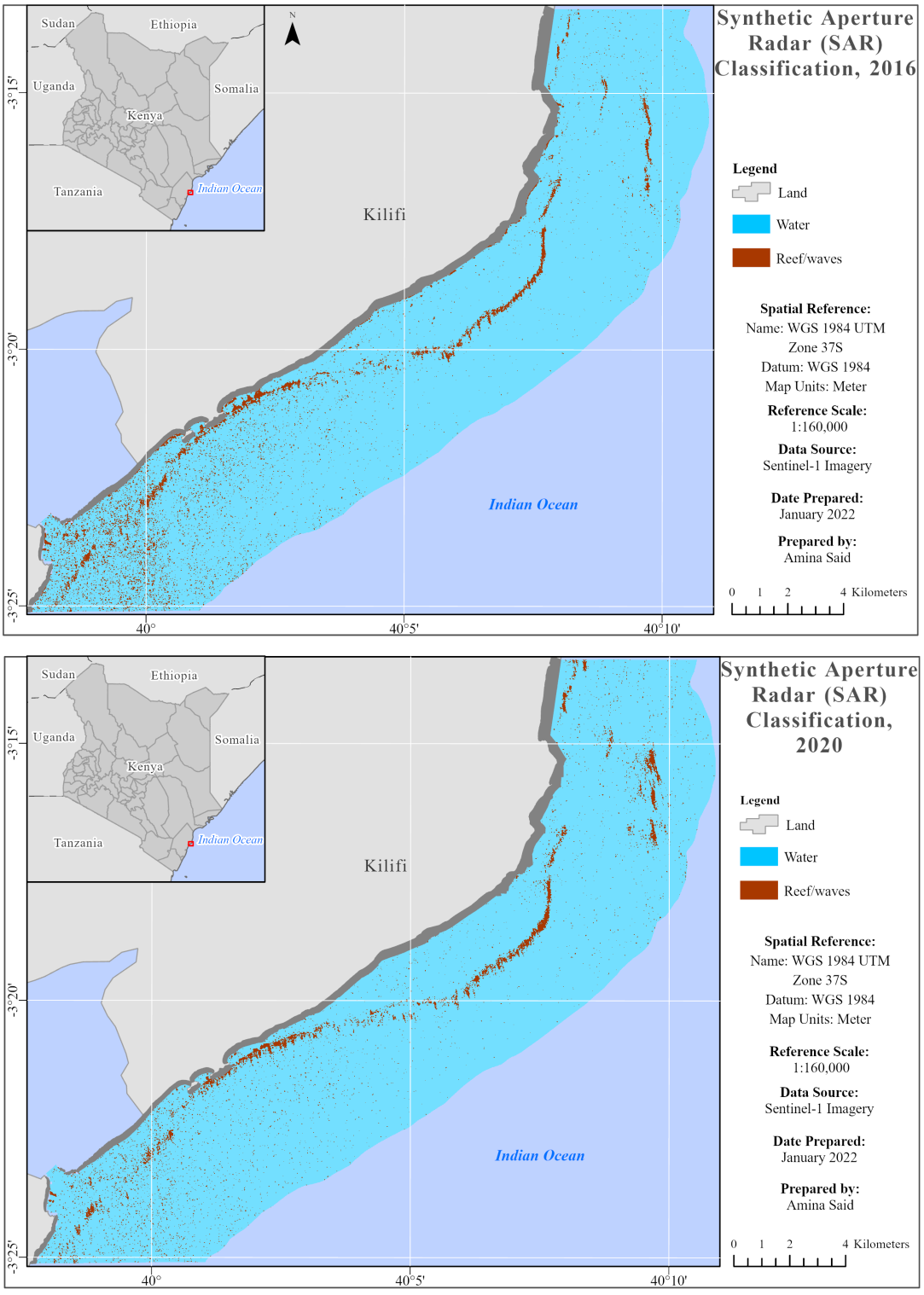

Figure 7. Change analysis of SAR between 2016 and 2020.

Sea surface is commonly unstill, which affects the backscattering values of SAR data. Thus, change detection is carried out to ascertain presence of exposed reefs. The change analysis indicates no change of exposed coral reefs. Hence, the feature

is not influenced by varying oceanic tides. Furthermore, this overcomes the doubt of having a temporary feature from being misclassified as emergent reef. As backscatter of exposed reefs are expected to be consistent or have a slight variation between the years.

4.4. Multispectral Classification

The initial processing is carried out on Sentinel-2 of 2016, to convert the data from TOA to BOA as previously discussed. Unfortunately, band-1 is eliminated from the atmospherically corrected bands during the atmospheric processing. Geometric pre-processing reduces the bulkiness of data as well as pixels inconsistency. Thus, sub-setting of the imagery improves processing speed of data. It also reduces data bulkiness and as a result less storage space is utilised. Moreover, resampling of pixels ensures the pixels are consistent and maintains data fidelity. Furthermore, radiometric correction enhances the visual appearance of features on imagery. This is done by reducing the atmospheric and environmental noise and biases, which ultimately eases discrimination of various marine features.

The water column correction (DII) assists in improving classification results of the shallow water features. This is by diminishing reflectance biases due to differences of depth of submerged features. It is observed that band-2 (blue) and band3 (green) have a good capability in mapping of shallow water marine features.

The results from OBIA classification method are not good, as it generalizes most of segments based on neighbourhood. This is attributed to the spatial resolution of the imagery. It is recommended to use OBIA when the benthic features to be mapped are larger than the spatial resolution of the imagery (Yuval et al., 2021). For this study, the spatial resolution used is 10 m. This may have contributed to the poor results. Moreover, some coral reefs are sparsely distributed and for some areas there is a mixture of seagrass and coral reefs. Other than the coral reefs and seagrass appearing geometrically close together, their spectral reflectance are also similar. Thus, affects the segmentation and classification results.

The reflectance of coral reefs and seagrass have a close association, which makes it challenging to separate the two features in classification. Hence, the training data used for OBIA could be biased due to the close spectral reflectance. Therefore, unsupervised classification is considered to resolve the supervised training biases of reflectance of the two features. Results of unsupervised classification of both water column corrected and uncorrected imageries show that multispectral imagery has better results as compared to results from DII. On analysing the classification result from fusion of MS imagery and DII, the result from the fused data proves to improve the accuracy of the classification results. Also, it is recognised that K-Means classifier presents better results as compared to EM-Cluster classifier. With better spatial and spectral resolution, results can improve and more features may be further classified. **Figure 8** shows the distribution of the shallow water benthic features classified.

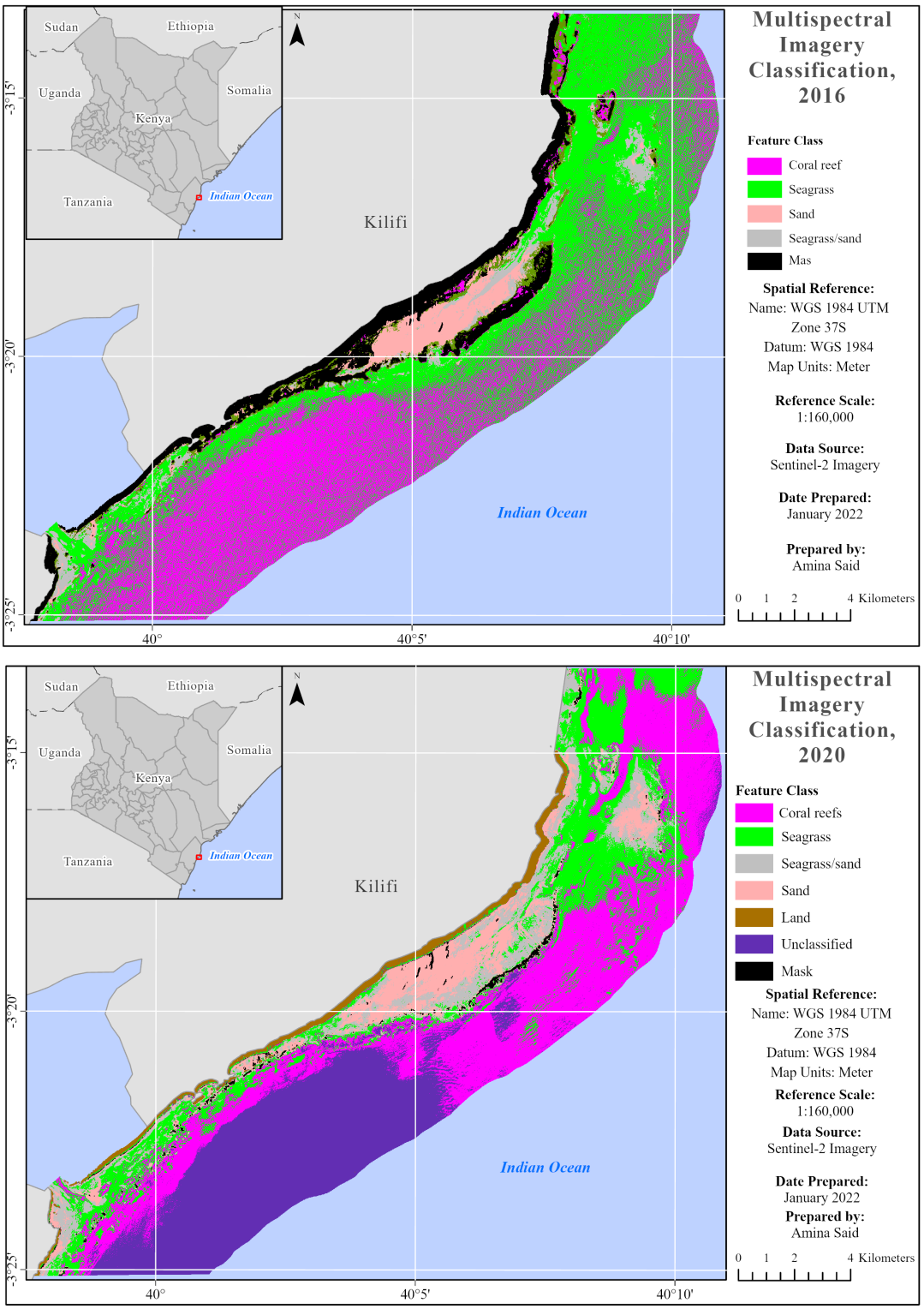

Figure 8. Classification of multispectral imageries in 2016 and 2020.

Though a similar trend of distribution of features is seen, the results of the two years have a difference in classification of seagrass and coral reefs. Classification results of 2020 have less noise and the delineation of coral reefs and seagrass is

clearly visible. While for 2016, there is a lot more mixture of coral type of coral reefs present in an area.

Out of the 64 random stratified samples, 37 and 40 points fall on the study area for 2016 and 2020 respectively. The difference of 3 samples of 2016 and 2020, is due to the points falling on a masked area of 2016. As the spatial extent of the study area is relatively small with approximately 169 km^2, the importance is ensuring the features and various parts of the study area are well covered by samples. However, more focus is on coral reefs and seagrass as the features tend to have more resemblance, hence more prone to classification errors.

The overall accuracy is approximately 68 and 83 percent for classification of 2016 and 2020 respectively. Moreover, the kappa coefficient of 2016 is lower than of 2020, with coefficient value of 0.5 and 0.7 respectively. The user's and producer's accuracy of coral reefs for 2016 is the same with 69 percent. While for 2020, the user's and producer's accuracy of coral reefs is 76 and 93 percent respectively.

In summary, the confusion matrix shows that the classification results of 2020 are more reliable as compared to 2016. However, the validation data may have an influence over the accuracy differences. Since the validation data is from 2018-2020. A lot may have changed between 2016 and the period in which the validation data was acquired. Table 2 and Table 3 show the confusion matrix for 2016 and 2020 respectively.

Table 2. Confusion matrix for accuracy assessment—2016.

	Reference data				
Classified data	Coral reef	Seagrass	Sand	Sum	UA (%)
Coral reefs	9	4	0	13	69.23
Seagrass	4	10	4	18	55.56
Sand	0	0	6	6	100.00
Sum	13	14	10	37	
PA (%)	69.23	71.43	60.00		
Overall accuracy = 69.23%					
Kappa coefficient = 0.5000					

Table 3. Confusion matrix for accuracy assessment—2020.

	Reference data				
Classified data	Coral reef	Seagrass	Sand	Sum	UA (%)
Coral reefs	13	3	1	17	76.47
Seagrass	1	11	2	14	78.57
Sand	0	0	9	9	100.00
Sum	14	14	12	40	
PA (%)	92.86	78.57	60.00		
Overall accuracy = 82.50%					
Kappa coefficient = 0.7353					

The difference of classification accuracies between 2016 and 2020 is linked to three factors. Firstly, classification results from 2020 utilise five bands of MS imagery i.e., band-1 to band-5. While for 2016, it uses a total of 4 band. That is band2 to band-5, as band-1 is eliminated after atmospheric correction. Secondly, the surface of water is more unstill in 2016 as compared to 2020. Gallagher et al. (2016) found that physical phenomena of water affect the underwater visibility due to resuspension of surface sediments which triggers water turbidness. Despite the sun deglint processing, the sun glint effects are still visible in MS imagery of 2016, which in return affects reflectance values, as well the classification results. Thirdly, the imagery of 2020 has a better water clarity as compared to imagery of 2016. This is linked to differences of climatic and environmental conditions, which affect the light penetration into water and subsequent visibility of features. The imagery of 2016 is captured not only during a hot season, but also during an El Nino event of 2015/2016 as previously discussed. Moreover, the water quality parameters are higher in 2016 as compared to 2020, which affects the detection of features by the satellite.

Nevertheless, it has been found that classification results of sea bottom surfaces tend to have lower accuracy as compared to mapping of land features (Teruhisa, 2015). This is due to the effects of water covering the submerged features. Furthermore, it is reported that the economical source of data relates inversely with the data resolution. That is, coarse resolution is expected with freely available data. This eventually directly influences classification results and accuracy. Thus, overall accuracy ranging between 60 - 80 percent is reasonable for mapping of coral reefs and seagrass (Mumby, Green, Edwards, & Clark, 1999). In summary, the overall accuracies of this study are relatively good, considering all the conditions stated above.

4.5. Multispectral Classification Correlation

No significant correlation is found between the DII with water quality parameters and SST. All the three correlation coefficients of 2016 are much lower as compared to 2020. The reason could be due to the higher chlorophyll and TSM concentrations, which affects detection of features, due to poor visibility as has been previously discussed.

A correlation is observed to exist between the TSM and chlorophyll concentration values. Hence regression analysis is carried out to evaluate the relationship that exists between TSM and chlorophyll concentrations. **Figure 9** and **Figure 10** show the regression curves for the year 2016 and 2020.

Figure 9 and **Figure 10** show a strong positive correlation between the concentration value of TSM and chlorophyll for both temporal periods. The correlation coefficient, R^2 for 2016 and 2020 is approximately 0.77 and 0.88 respectively. However, the correlation is more significant in 2020 as compared to 2016. Thus, the TSM values maybe used to predict the chlorophyll concentration values, however more research needs to be carried out to analyse further the correlation and may

consider adding more variables such as SST. This will assist in understanding the relationship of the two parameters, which may further assist in using the variables for prediction and assist in modelling of the changes and variations.

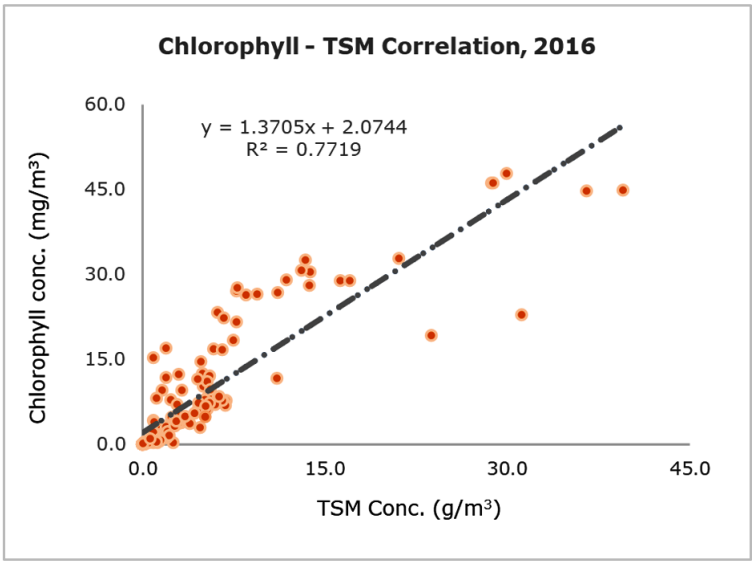

Figure 9. TSM and chlorophyll correlation, 2016.

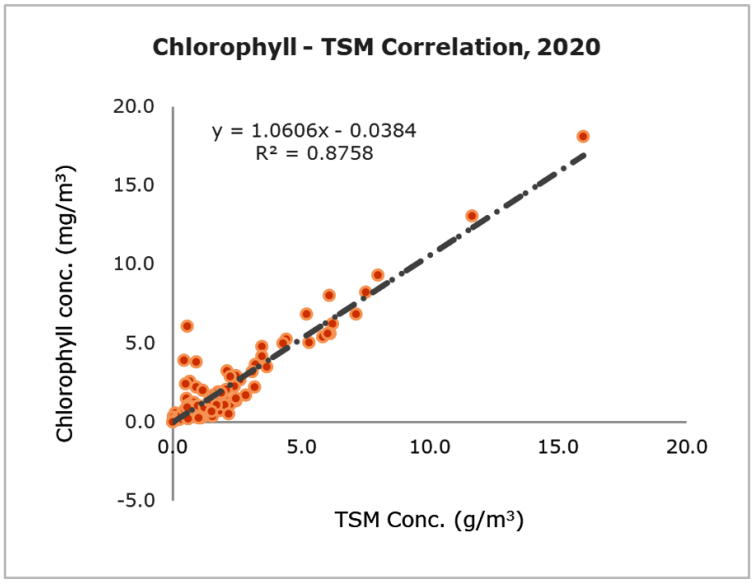

Figure 10. TSM and chlorophyll correlation, 2020.

5. Conclusion and Recommendation

5.1. Conclusion

The study affirms the capability of mapping coral reefs using multispectral and SAR imageries. The overall accuracy of both temporal periods is relatively good, approximately 68 and 83 percent for 2016 and 2020 respectively. Thus, remote sensing can be utilised to identify the type of coral reefs based on the pattern and

trend identified on the satellite imagery. Moreover, the study shows that there is a good consistency of using C2RCC in retrieving water quality parameters. A good RMSE value of less than 3 units per cubic metre is attained in this study, despite the difference of spatial resolution of Sentinel-2 and MODIS-Terra/Sentinel-3. The RMSE of SST between the Landsat-8 and validation data, i.e., GHRSST is approximately one degree, which confirms previous studies on reliability of satellite imageries in estimation of surface temperatures. The water quality parameters fluctuations are small and may be due to natural reasons and not anthropogenic causes. The study demonstrates that the efforts by KWS in protecting and managing the MPAs are fruitful, which gives hope for realization of the SDG of protecting the coast and marine areas.

5.2. Recommendation

Hyperspectral imagery and high spatial resolution imageries maybe used in mapping of coral reefs. With high spatial resolution imagery of pixel size smaller than coral reef size, will assist in better classification. With extensive distribution of coral reefs or better spatial resolution, OBIA may be considered to improve the segmentation and classification.

Additionally, more features may be discriminated. Moreover, integration of various remote sensing techniques may be used to facilitate mapping at different scale and resolution. That is, satellite data may be used to provide a general coral reef map. This can then be complemented by utilising UAVs and underwater cameras of high spatial and spectral resolution to provide detailed coral maps with 3D models. Fusion of various geospatial data may be considered to provide detailed and more accurate coral reef maps.

Lastly, more studies need to be carried out to analyse and understand the correlation of DII to various environmental and climatic conditions. These studies may focus on small scale, to ensure it is representative and cover heterogeneous marine areas. This will assist in not only monitoring, but as well as identifying the cause of the variation for corresponding mitigation measure.

Conflicts of Interest

The authors declare no conflicts of interest regarding the publication of this paper.

References

Budi Cahyono, A., Wibisono, A. C., Saptarini, D., Permadi, R. I., Budisusanto, Y., & Hidayat, H. (2020). Underwater Photogrammetry Application for Coral Reef Mapping and Monitoring. *International Journal on Advanced Science, Engineering and Information Technology, 10,* 293-297. https://doi.org/10.18517/ijaseit.10.1.6747

Casella, E., Collin, A., Harris, D., Ferse, S., Bejarano, S., Parravicini, V. et al. (2017). Mapping Coral Reefs Using Consumer-Grade Drones and Structure from Motion Photogrammetry Techniques. *Coral Reefs, 36,* 269-275. https://doi.org/10.1007/s00338-016-1522-0

Chin, T. M., Vazquez-Cuervo, J., & Armstrong, E. M. (2017). A Multi-Scale High-Resolution

Analysis of Global Sea Surface Temperature. *Remote Sensing of Environment, 200,* 154-169. https://doi.org/10.1016/j.rse.2017.07.029

CIAT (2016) *Kenya County Climate Risk Profile: Kilifi County*. CIAT. https://cgspace.cgiar.org/bitstream/handle/10568/80453/Kilifi.pdf?se-quence=5&isAl-lowed=y

Conservation Education Society (2021) *Coral Reefs in Kenya*. https://ceskenya.org/coral-reefs-in-kenya/

Coral Reef Alliance (2021) *Coastal Protection*. https://coral.org/coral-reefs-101/why-care-about-reefs/coastal-protection/

Daud, M., Pin, T. G., & Handayani, T. (2019). The Spatial Pattern of Seagrass Distribution and the Correlation with Salinity, Sea Surface Temperature, and Suspended Materials in Banten Bay. *IOP Conference Series: Earth and Environmental Science, 243,* Article 012013. https://doi.org/10.1088/1755-1315/243/1/012013

Filipponi, F. (2019). Sentinel-1 GRD Preprocessing Workflow. *Proceedings, 18,* Article 11. https://doi.org/10.3390/ecrs-3-06201

Gallagher, J. B., Hoe, C. C., Yusob, M. S. B. M., Gen, C. N., & Mae, G. Y. (2016) Surface Chlorophyll Patchiness across Sepanggar Bay: Relationships with Turbidity and Depth. *Transactions on Science and Technology, 3,* 421-426.

Gomez, A. M., McDonald, K. C., Shein, K., DeVries, S., Armstrong, R. A., Hernandez, W. J. et al. (2020). Comparison of Satellite-Based Sea Surface Temperature to in Situ Observations Surrounding Coral Reefs in La Parguera, Puerto Rico. *Journal of Marine Science and Engineering, 8,* Article 453. https://doi.org/10.3390/jmse8060453

Hedley, J. D., Harborne, A. R., & Mumby, P. J. (2005). Technical Note: Simple and Robust Removal of Sun Glint for Mapping Shallow-Water Benthos. *International Journal of Remote Sensing, 26,* 2107-2112. https://doi.org/10.1080/01431160500034086

Hoegh-Guldberg, O., Poloczanska, E. S., Skirving, W., & Dove, S. (2017). Coral Reef Ecosystems under Climate Change and Ocean Acidification. *Frontiers in Marine Science, 4,* Article 158. https://doi.org/10.3389/fmars.2017.00158

Kennedy, E. and CR, R. (2020) *Reef-Cover-Class-Definitions: Coral Reef Internal Class Descriptors for Global Habitat Mapping*. The University of Queensland Australia. https://reefresilience.org/wp-content/uploads/REEF-COVER-CLASS-DEFINI-TIONS.pdf

Korting, T. S., Dutra, L. V., Fonseca, L. M. G., Erthal, G., & da Silva, F. C. (2007) Improvements to Expectation-Maximization Approach for Unsupervised Classification of Remote Sensing Data. In *GeoINFO* (pp. 3-11).

La Yasir Haya, O. M., & Fujii, M. (2017). Mapping the Change of Coral Reefs Using Remote Sensing and in Situ Measurements: A Case Study in Pangkajene and Kepulauan Regency, Spermonde Archipelago, Indonesia. *Journal of Oceanography, 73,* 623-645. https://doi.org/10.1007/s10872-017-0422-4

Mumby, P. J., Green, E. P., Edwards, A. J., & Clark, C. D. (1999). The Cost-Effectiveness of Remote Sensing for Tropical Coastal Resources Assessment and Management. *Journal of Environmental Management, 55,* 157-166. https://doi.org/10.1006/jema.1998.0255

NASA Earth Observatory (2017) *El Niño: Pacific Wind and Current Changes Bring Warm, Wild Weather*. https://earthobservatory.nasa.gov/features/ElNino

Nima, C., Frette, Ø., Hamre, B., Erga, S. R., Chen, Y., Zhao, L. et al. (2016). Absorption Properties of High-Latitude Norwegian Coastal Water: The Impact of CDOM and Particulate Matter. *Estuarine, Coastal and Shelf Science, 178,* 158-167. https://doi.org/10.1016/j.ecss.2016.05.012

NOAA (2021) *In What Types of Water Do Corals Live?* https://oceanservice.noaa.gov/facts/coralwaters.html

Park, J., Korosov, A. A., Babiker, M., Sandven, S., & Won, J. (2018). Efficient Thermal Noise Removal for Sentinel-1 TOPSAR Cross-Polarization Channel. *IEEE Transactions on Geoscience and Remote Sensing, 56,* 1555-1565. https://doi.org/10.1109/tgrs.2017.2765248

Rudorff, F. M., & Gherardi, D. F. M. (2008). Coral Reef Detection Using SAR/RADARSAT-1 Images at Costa Dos Corais, PE/AL, Brazil. *Brazilian Journal of Oceanography, 56,* 85-96. https://doi.org/10.1590/s1679-87592008000200002

Sent, G., Biguino, B., Favareto, L., Cruz, J., Sá, C., Dogliotti, A. I. et al. (2021). Deriving Water Quality Parameters Using Sentinel-2 Imagery: A Case Study in the Sado Estuary, Portugal. *Remote Sensing, 13,* Article 1043. https://doi.org/10.3390/rs13051043

Teruhisa, K. (2015) *A Manual for Seagrass and Seaweed Beds Distribution Mapping with Satellite Images*.

USGS (2022) *How DO I use a Scale Factor with Landsat Level-2 Science Products*. https://www.usgs.gov/faqs/how-do-i-use-scale-factor-landsat-level-2-science-products

Yuval, M., Alonso, I., Eyal, G., Tchernov, D., Loya, Y., Murillo, A. C. et al. (2021). Repeatable Semantic Reef-Mapping through Photogrammetry and Label-Augmentation. *Remote Sensing, 13,* Article 659. https://doi.org/10.3390/rs13040659

Zanga, H., Boraski, A., & Olendorf, A. (2019) *A Student's Guide to Tropical Marine Biology*. Keene State College. https://karencang.net/wp-content/uploads/2019/12/A-Student039s-Guide-to-Tropical-Marine-Biology-1576764955.pdf